

# Substitution of the Laser Borane *anti*-B<sub>18</sub>H<sub>22</sub> with Pyridine: A Structural and Photophysical Study of some Unusually Structured Macropolyhedral Boron Hydrides

Michael G. S. Londesborough,<sup>1</sup> Jiří Dolanský,<sup>1,2</sup> Tomáš Jelínek,<sup>1,3</sup> John D. Kennedy,<sup>1,4</sup> Ivana Cisařová,<sup>2</sup> Robert D. Kennedy,<sup>4</sup> Daniel Roca-Sanjuán,<sup>5</sup> Antonio Francés-Monerris,<sup>5</sup> Kamil Lang,<sup>1</sup> and William Clegg.<sup>6</sup>

<sup>1</sup> Institute of Inorganic Chemistry of the Czech Academy of Sciences, v.v.i., 250 68, Husinec-Řež, Czech Republic.

<sup>2</sup> Charles University in Prague, Department of Inorganic Chemistry, Hlavova 2030/8, 128 43 Prague 2, Czech Republic.

<sup>3</sup> Katchem s.r.o., pracoviště Minická 635, 278 01 Kralupy nad Vltavou, Czech Republic.

<sup>4</sup> The School of Chemistry of the University of Leeds, Leeds UK LS2 9JT.

<sup>5</sup> Instituto de Ciencia Molecular, Universitat de València, P.O. Box 22085, ES-46071, València.

<sup>6</sup> The School of Chemistry of Newcastle University, Newcastle upon Tyne UK NE1 7RU.

## Content

- SI 1.** Selected crystallographically determined interatomic distances for the molecular structure of  $B_{18}H_{20}Py_2$  **2**.
- SI 2.** Simple factorisation of the electronic structure of compound **2**.
- SI 3.** Selected crystallographically determined interatomic distances for the molecular structure of  $B_{16}H_{18}Py_2$  **3a** and  $B_{16}H_{18}Pic_2$  **3b**.
- SI 4.** Molecular structure of **3b**.
- SI 5.** Selected measured  $^{11}B$  and  $^1H$  NMR parameters for  $B_{16}H_{18}(NC_6H_4-4-isoPr)_2$  (compound **3c**) and  $B_{16}H_{18}(NC_6H_4-4-Me)_2$  (compound **3b**) in  $(CD_3)_2CO$  solution at *ca.* 293 K, together with their tentative assignments.
- SI 6.** Selected crystallographically determined interatomic distances for the molecular structure of  $B_{18}H_{20}Py$  **4**.
- SI 7.** Measured  $^{11}B$  and  $^1H$  NMR chemical shifts and tentative assignments for *anti*- $B_{18}H_{20}-8'$ -Py (compound **4**);  $CD_2Cl_2$  solution.
- SI 8.** Comparison  $^{11}B$  and  $^1H$  NMR chemical shifts and assignments for neutral  $[5'-\{(MeNH)C_3N_2HMe_2\}-anti-B_{18}H_{20}]$  and for the  $[anti-B_{18}H_{21}]^-$  anion.
- SI 9.** Crystal structure diagram for compound **3b**.
- SI 10.** CASSCF natural orbitals that compose the CAS active space of  $B_{18}H_{20}Py$ , compound **4**, at the  $(S_0)_{min}$  structure.
- SI 11.** Full rationale for the absorption characteristics of compound **4**.
- SI 12.** CASSCF natural orbitals that compose the CAS active space of  $B_{16}H_{18}Py_2$ , compound **4**, at the  $(S_0)_{min}$  structure.

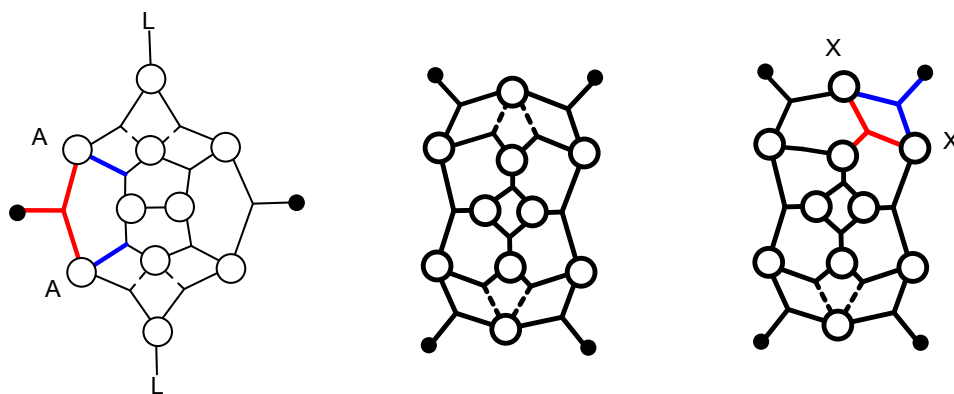
## References

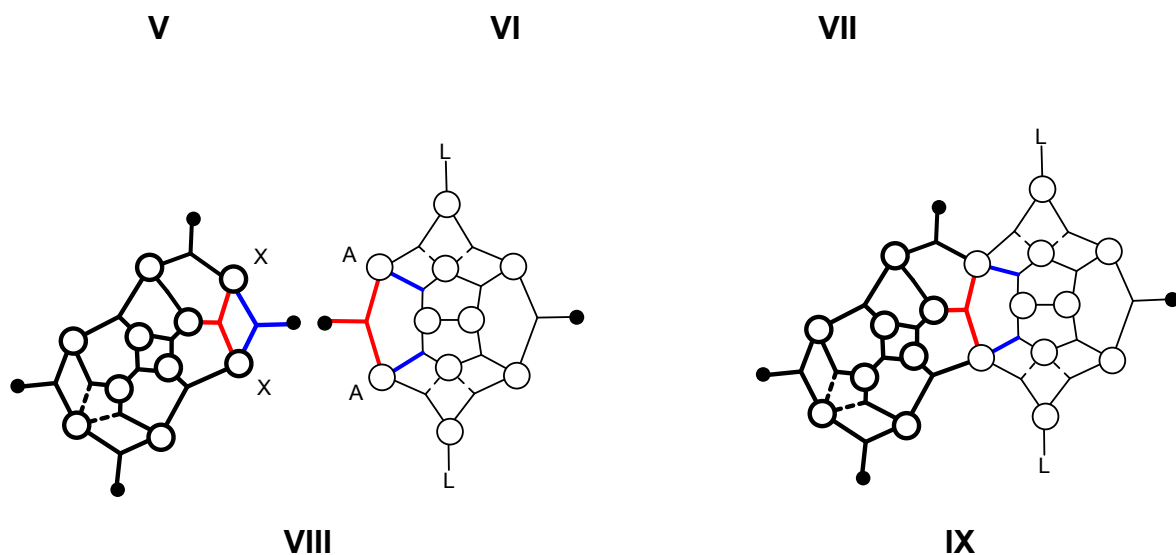
**SI 1.** Selected crystallographically determined interatomic distances for the molecular structure of  $B_{18}H_{20}Py_2$  **2**; additional values may be found in the crystallographic cif file.

B5-B6	1.870(2)	B6'-N61	1.566(2)
B5-B10	2.007(2)	B9'-N91	1.568(2)
B6-B7	1.851(2)	B5-B9'	1.935(2)
B7-B8	1.919(2)	B8'-B9'	1.851(2)
B8-B9	1.814(3)	B7'-B8'	1.880(2)
B9-B10	1.797(2)	B6'-B7'	1.835(2)
		B6-B6'	1.899(2)

**SI 2.** Simple factorisation of the electronic structure of compound **2**.

Rationalisation of the overall electronic structure of compound **2** can be found by reference to simple Lipscomb-type semi-localised bonding schemes<sup>a,b</sup> of its constituent conjoined two subclusters. Such representations for compound **5** and  $B_{10}H_{14}$  are in *schematic bonding diagrams V* and *VI* respectively. For the two-atoms-in-common cluster fusion mode, a common instance is when the B-H-B three-centre bridge of one subcluster model mimics the B-B-B three-centre bond in the other subcluster model, and the latter formally replaces the former.<sup>c,d</sup> In order to accommodate this, the partial three-centre bonding character within the *nido*-decaboranyl subcluster **VI** needs to be localised into one two-centre and one three-centre bond (schematic **VII**). This breaks the bonding symmetry and thence significantly perturbs the internal molecular orbital structure; this change in internal ‘intracluster’ bonding will change the chemical properties of the cluster. The formal B-B-B fusion replacement of B-H-B then models a bonding description for compound **5** (Schematics **VIII** and **IX**). It can be seen that the electronic structure of the *arachno* subcluster retains its single-cluster characteristics, in contrast to that of the *nido* residue, which is perturbed near the site of fusion.



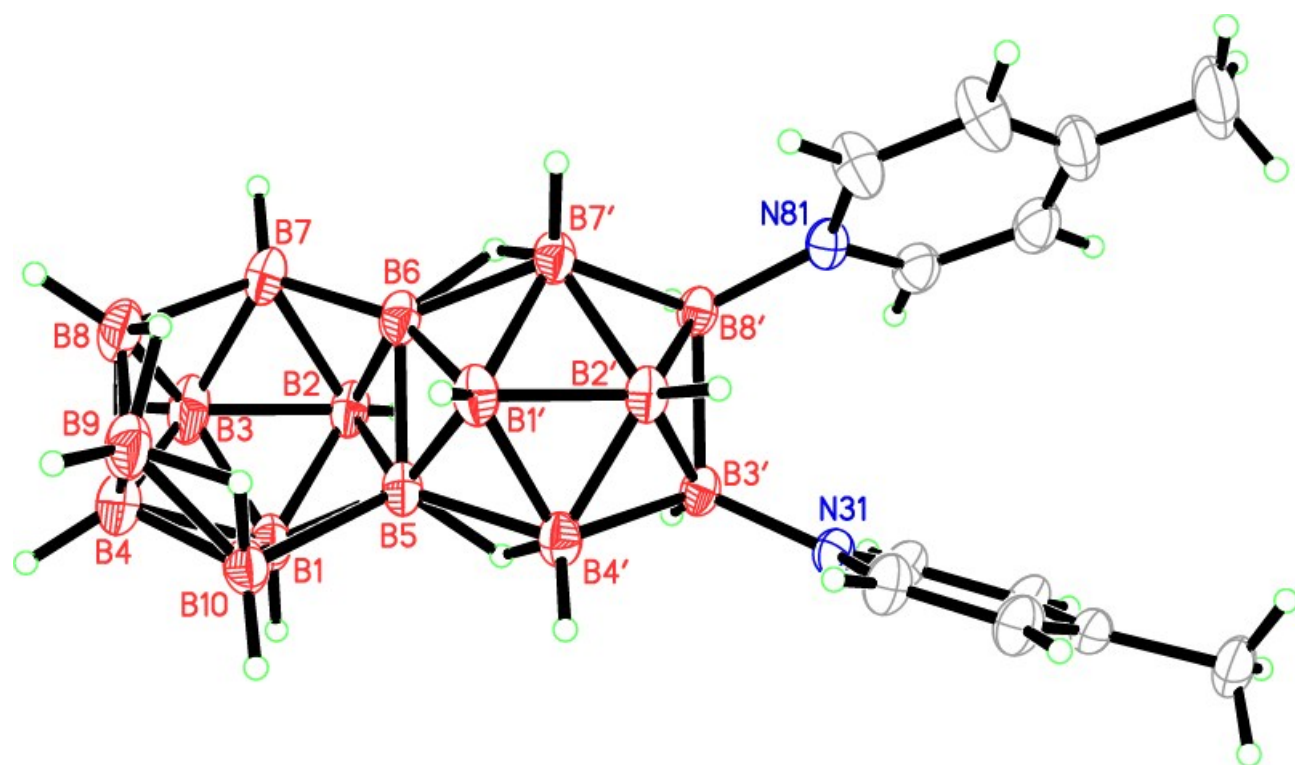


**SI 3.** Selected crystallographically determined interatomic distances for the molecular structure of  $B_{16}H_{18}Py_2$  **3a** and  $B_{16}H_{18}Pic_2$  **3b**; additional values may be found in the crystallographic cif files.

	<b>3a</b>	<b>3b</b>		<b>3a</b>	<b>3b</b>
B5-B6	1.777(4)	1.781(3)	B3'-N31	1.566(3)	1.563(2)
B5-B10	1.899(4)	1.942(4)	B8'-N81	1.571(3)	1.565(2)
B6-B7	1.658(5)	1.692(3)	B5-B4'	1.830(3)	1.832(3)
B7-B8	1.850(6)	1.819(4)*	B7'-B8'	1.894(3)	1.885(3)
B8-B9	1.800(7)	1.856(7)*	B3'-B4'	1.882(3)	1.874(3)
B9-B10	1.774(5)	1.785(6)	B3'-B8'	1.885(4)	1.911(3)
			B6-B7'	1.806(4)	1.807(3)

\*these crystallographically derived distances for **3b** severely affected by crystallographic disorder.

SI 4. Molecular structure of **3b**.



**SI 5.** Selected measured  $^{11}\text{B}$  and  $^1\text{H}$  NMR parameters for  $\text{B}_{16}\text{H}_{18}(\text{NC}_6\text{H}_4\text{-4-isoPr})_2$  (compound **3c**) and  $\text{B}_{16}\text{H}_{18}(\text{NC}_6\text{H}_4\text{-4-Me})_2$  (compound **3b**) in  $(\text{CD}_3)_2\text{CO}$  solution at *ca.* 293 K, together with their tentative assignments.

Assignment	$\text{B}_{16}\text{H}_{18}(\text{NC}_6\text{H}_4\text{-4-isoPr})_2$ <b>3c</b>		$\text{B}_{16}\text{H}_{18}(\text{NC}_6\text{H}_4\text{-4-Me})_2$ <b>3b</b>	
	$\delta(^{11}\text{B})/\text{ppm}$	$\delta(^1\text{H})/\text{ppm}$	$\delta(^{11}\text{B})/\text{ppm}$	$\delta(^1\text{H})/\text{ppm}$
B(6)	+21.8	<i>conjuncto</i> site	+21.7	<i>conjuncto</i> site
BH(3)	+4.1	+2.94	+4.0	+2.95
BH(10)	+1.1	+3.13	<i>ca.</i> +0.9	+3.13
BH(2')	+0.2	+3.21	-0.12	+3.25
B(5)	-6.5	<i>conjuncto</i> site <i>ca.</i>	-7.0	<i>conjuncto</i> site
BH(1)(8) and (9)	<i>ca.</i> -8.5	+2.62	<i>ca.</i> -8.5	+2.59
	<i>ca.</i> -8.5	+2.11	<i>ca.</i> -8.5	+2.28
	<i>ca.</i> -8.5	+2.56	<i>ca.</i> -8.5	+2.59
BH(7)	-10.1	+2.48	-10.1	+2.50
BH(8')	-15.4	+2.28	-15.5	+2.34
BH(3')	-18.6	+1.98	-18.7	+2.00
BH(7)	-23.8	+2.02	-23.9	+2.00
BH(4')	-26.9	+1.60	-27.0	+1.58
BH(2)	-27.8	-0.63	-27.7	-0.62
BH(4)	-43.2	+0.19	-43.3	+0.20
BH(1')	-46.0	-1.25	-46.1	-1.23
mH(6,7')	-	-1.74		-1.71
mH(9,10)	-	-1.74		-1.71
mH(8,9)	-	-2.86		-2.84
mH(5,4')	-	+0.82		+0.85
C6H4	-	+7.6 (4H), +8.6 (4H)	+7.6 (4H), +8.6 (4H)	
CH		+2.92 (2H)		-
Me		+1.27 (12H)		+2.54(6H)

**SI 6.** Selected crystallographically determined interatomic distances for the molecular structure of B<sub>18</sub>H<sub>20</sub>Py **4**; additional values may be found in the crystallographic cif file.

B5-B6	1.807(2)	B8'-N81	1.549(2)
B5-B10	1.969(2)	B5'-B10'	2.037(3)
B6-B7	1.834(2)	B5-B5'	1.814(2)
B7-B8	1.950(2)	B6-B8'	1.831(2)
B8-B9	1.807(2)	B8'-B9'	1.650(2)
B9-B10	1.782(2)	B9'-B10'	1.784(2)

**SI 7.** Measured <sup>11</sup>B and <sup>1</sup>H NMR chemical shifts and tentative assignments for *anti*-B<sub>18</sub>H<sub>20</sub>-8'-Py (compound **4**); CD<sub>2</sub>Cl<sub>2</sub> solution.

Provisional assignment	δ( <sup>11</sup> B)	δ( <sup>1</sup> H)	correlations with μH
BH(4)	-42.9	+0.18	
BH(4')	-35.8	-0.06*	
BH(2)	-32.1	-0.06*	
BH(2')	-30.0	+0.61	
BH	-20.2	+2.20	μH -1.44
BH(7)	-17.0	+2.56	μH -0.42
BH	-15.5	+1.99	
BH	-6.9	-	μH -1.44
B	-4.4	-	μH -2.77
BH(1)	-0.6	+3.05	
BH(9)	+0.3	+3.41	μH -2.77, +0.01
BH	+1.4	+3.78	μH -2.43
B, BH (10), BH(6)	ca. +6.7**	-, +3.83, +3.41	μH -0.42, +0.01
B	+9.4	-	
BH(3)	+10.7	-3.62	
BH(5)	+11.3	-	

Notes: \* two <sup>1</sup>H resonances by chance coincident. \*\* Three <sup>11</sup>B resonances by chance coincident.

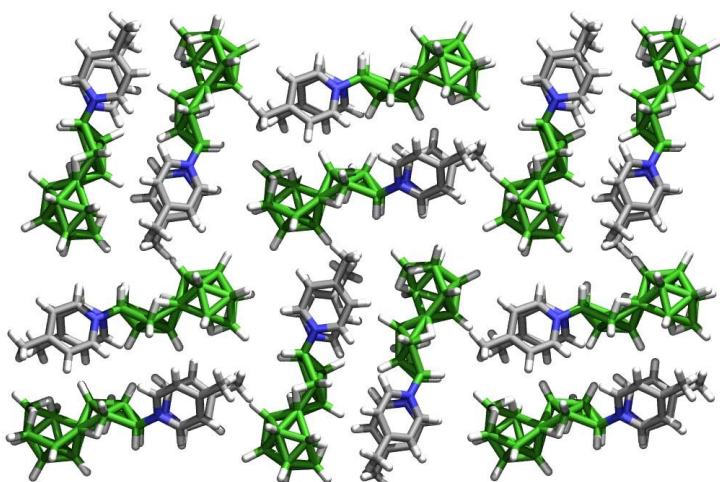
**SI 8.** Comparison  $^{11}\text{B}$  and  $^1\text{H}$  NMR chemical shifts and assignments for neutral  $[\text{5}'\text{-}\{(\text{MeNH})\text{C}_3\text{N}_2\text{HMe}_2\}\text{-anti-B}_{18}\text{H}_{20}]$  (data from reference 6) and for the  $[\text{anti-B}_{18}\text{H}_{21}]^-$  anion (data from reference 16).

Assignment <sup>6,16</sup>	$[\{(\text{MeNH})\text{C}_3\text{N}_2\text{HMe}_2\}\text{B}_{18}\text{H}_{20}]^*$		$[\text{anti-B}_{18}\text{H}_{21}]^-$ anion <sup>**</sup>	
	$\delta(^{11}\text{B})/\text{ppm}$	$\delta(^1\text{H})/\text{ppm}$	$\delta(^{11}\text{B})/\text{ppm}$	$\delta(^1\text{H})/\text{ppm}$
BH(1)	-3.4	+2.72	-4.5	+2.64
BH(2)	-29.5	-0.89	-29.2	-0.92
BH(3)	+13.5	+3.55	+13.4	+3.50
BH(4)	-38.9	+0.19	-41.1	+0.17
BH(5/6')	+15.3	<i>conjuncto</i> site	+17.0	<i>conjuncto</i> site
BH(6,7')	-0.2	<i>conjuncto</i> site	+0.1	<i>conjuncto</i> site
BH(7)	-12.0	+2.80	-13.6	+2.62
BH(8)	-9.2	+2.55	-10.0	+2.44
BH(9)	-0.2	+2.90	-1.2	+2.94
BH(10)	+8.3	+3.20	+9.3	+3.73
BH(1')	+5.5	+3.21	+5.1	+2.98
BH(2')	-24.2	-0.01	-24.1	-0.42
BH(3')	-12.0	+1.90 or +2.20	-10.6	+2.11
BH(4')	-41.6	+0.32	-39.2	+0.19
BH(5')	-5.1	ligand site	-3.4	+2.76
BH(8')	+4.1	+3.65	+3.2	+3.51
BH(9'')	-7.6	+2.65	-7.7	+2.55
BH(10')	-12.0	+1.90 or +2.20	-13.0	+1.86
$\mu\text{H}(8,9)$		-2.92		-3.31
$\mu\text{H}(9,10)$		-1.23		-1.03
$\mu\text{H}(6/7',7)$		-1.80		-1.88
$\mu\text{H}(8',9')$		-1.38		-1.59
$\mu\text{H}(9',10')$		-3.60		-3.90

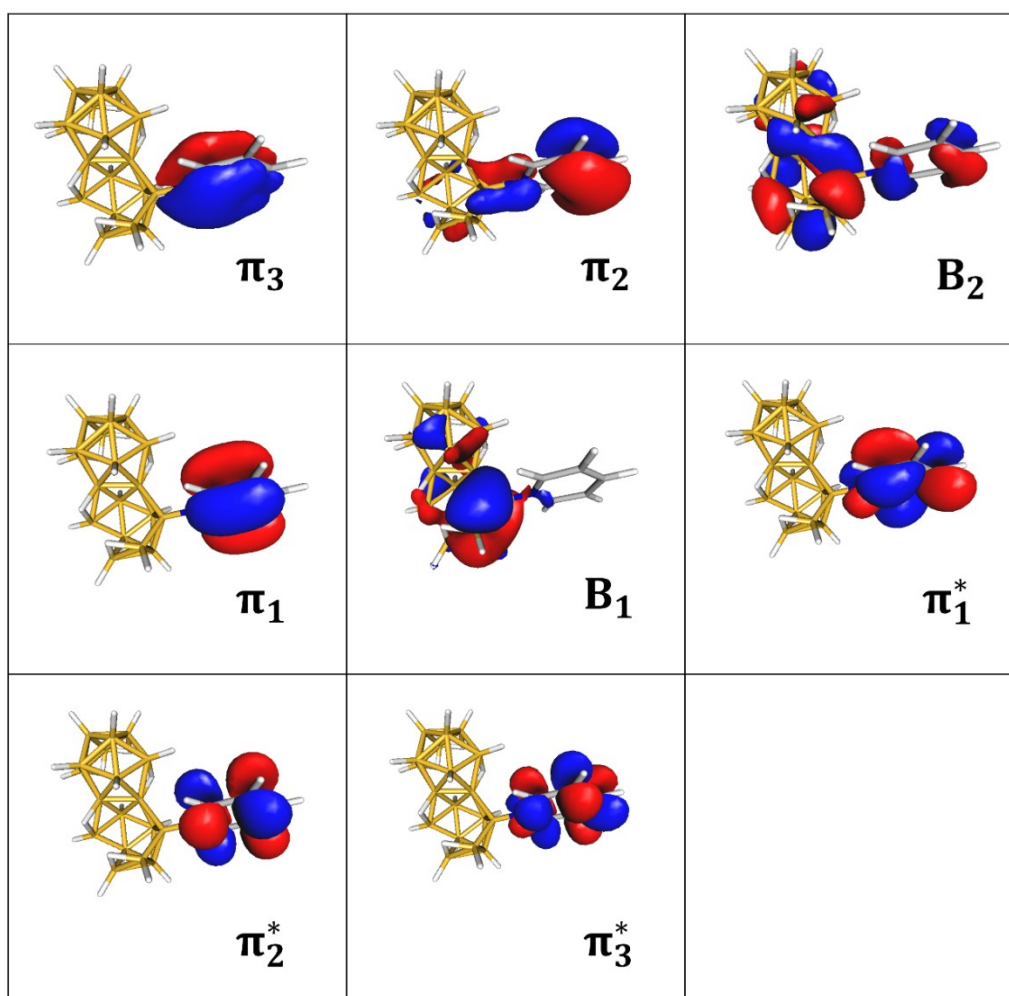
Notes: \* Ligand species:  $(\text{CD}_3)_2\text{CO}$  solution. \*\* Anion:  $\text{CD}_2\text{Cl}_2$  solution;  $[\text{C}_{10}\text{H}_6(\text{NMe}_2)_2\text{H}]^+$  salt.



SI 9. Crystal structure diagram for compound **3b**.



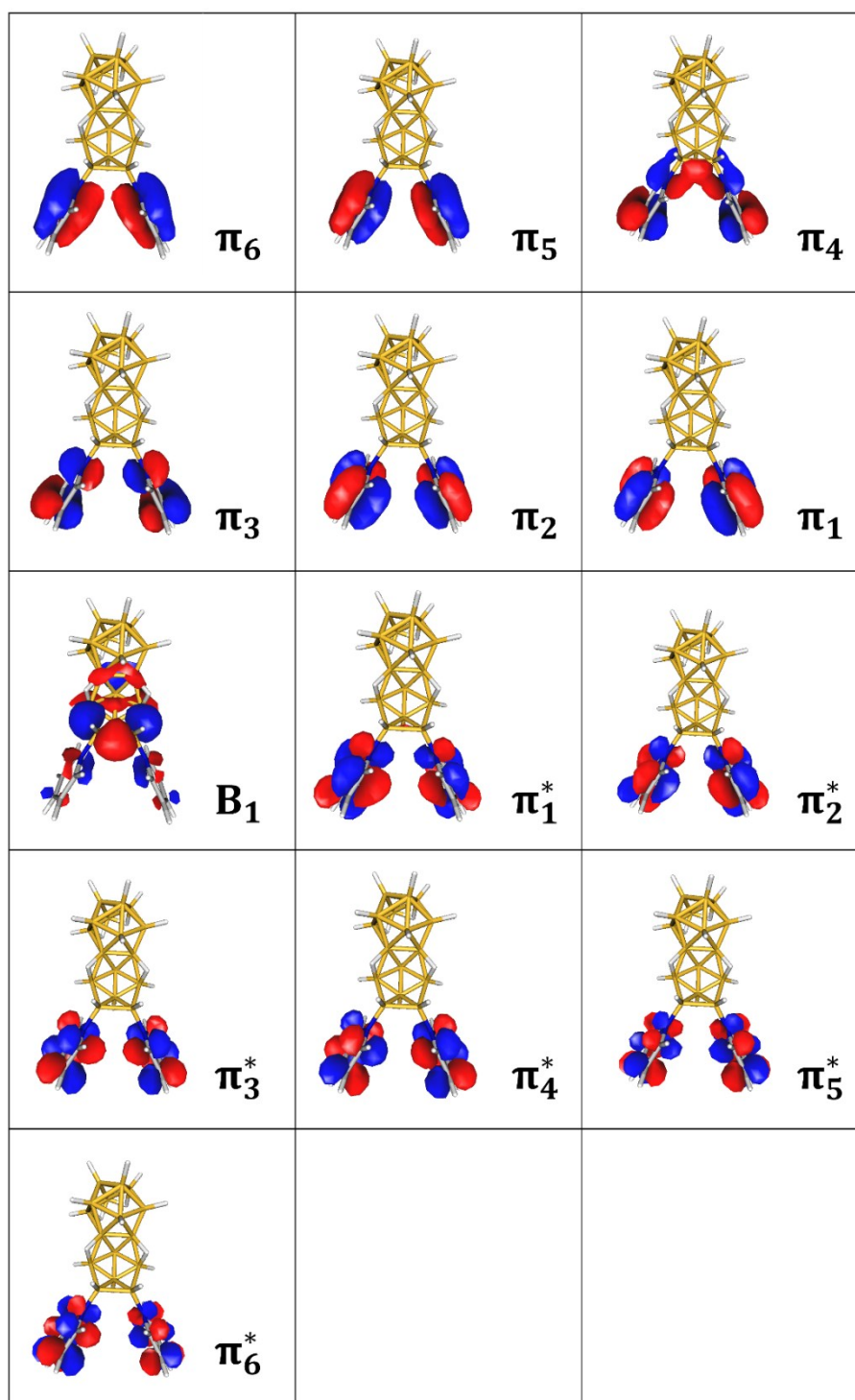
SI 10. CASSCF natural orbitals that compose the CAS active space of  $B_{18}H_{20}Py$ , compound **4**, at the  $(S_0)_{min}$  structure.



## SI 11. Full rationale for the absorption characteristics of compound 4.

The CASPT2(IPEA=0.25) calculated energy for the most probable electronic transition, 4.54 eV (273 nm), with an  $f$  of 0.2265, has a high value as compared to the experimentally measured absorption band with a band maximum recorded at 320 nm (see Figure 7). The lowest-energy transition computed at 3.69 eV (336 nm) has a much lower  $f$  value (0.0082). The calculation of more states (up to eight) and the use of the multi-state CASPT2 method,<sup>e</sup> which provides more correlated wave functions, do not change the scenario. CASPT2(IPEA=0.00) computations have been also carried out giving rise to vertical transition energies of 3.27 and 3.95 eV (379 and 314 nm) for the excitations to  $S_1$  and  $S_2$ , respectively. The  $f$  values are 0.0073 and 0.1972, respectively. Taking into account both group of values, we can assign the  $S_0 \rightarrow S_2$  electronic transition to the band maximum and the  $S_0 \rightarrow S_1$  one to the broad curve of the band appearing at lower energies. Meanwhile, transitions related to  $S_3$  and  $S_4$  might be responsible for the absorbance appearing in the 250-300 nm range. To be consistent with our previous work,<sup>f</sup> we continue the theoretical analysis on the photophysics of the system using the CASPT2(IPEA=0.25) level of theory. Even though this level shows a worse agreement with the experimental data as compared to the outcomes of the CASPT2(IPEA=0.00) level, the IPEA parameter only provides with a systematic shift of the energies and then the qualitative behavior is maintained.

SI 12. CASSCF natural orbitals that compose the CAS active space of  $B_{16}H_{18}Py_2$ , compound **4**, at the  $(S_0)_{min}$  structure.



## References

- a. See, for example, page 71 in W. N. Lipscomb, *Boron Hydrides*, Benjamin, New York and Amsterdam, 1963.
- b. See, for example, page 59 in E. L. Muetterties (Ed), *Boron Hydride Chemistry*, Academic, New York, San Francisco and London, 1975.
- c. L. Barton, J. Bould, J. D. Kennedy and N. P. Rath, *J. Chem. Soc., Dalton Trans.*, 1996, 3145-3149.
- d. S. L. Shea, P. I. MacKinnon, M. Thornton-Pett and J. D. Kennedy, *Inorg. Chim. Acta, Special Issue for Gordon Stone*, 2005, **358**, 1709-1714.
- e. J. Finley, P.-Å. Malmqvist, B. O. Roos, and L. Serrano-Andrés, *Chem. Phys. Lett.*, 1998, **228**, 299.
- f. M. G. S. Londesborough, J. Dolanský, L. Cerdán, K. Lang, T. Jelínek, I. Garcia-Moreno, J. M. Oliva, D. Hnyk, D. Roca-Sanjuán, J. Martinčík, M. Nikl, and J. D. Kennedy, *Adv. Opt. Mater.*, 2017, **5**, 1600694.